Snow persistence influences vegetation metrics central to Arctic greening analyses

Calum G. Hoad[1], Isla H. Myers-Smith[1,2], Jeff T. Kerby[3], Claudia Colesie[1], Jakob J. Assmann[4]

Corresponding author email: calum.hoad@ed.ac.uk

[1] University of Edinburgh, [2] University of British Columbia, [3] Scott Polar Research Institute, [4] University of Zurich

Key words: Arctic greening, snow, spatial resolution, NDVI, drones, plants, phenology

Abstract

Satellite imagery is critical for understanding land-surface change in the rapidly warming Arctic. Since the 1980s, studies have found positive trends in the normalised difference vegetation index (NDVI) derived from satellite imagery over the Arctic - commonly referred to as *'Arctic greening'* and assumed to represent increased vegetation productivity. However, greening analyses use satellite imagery with pixel sizes ranging from tens to hundreds of metres and do not account for the integration of abiotic phenomena such as snow within vegetation indices. Here, we use high resolution drone data from one Arctic and one sub-Arctic site to show that fine-scale snow persistence within satellite pixels is associated with both reduced magnitude and delayed timing of annual peak NDVI, the base metric of Arctic greening analyses. We found higher snow persistence within Sentinel-2 pixels is associated with a lower magnitude and later peak NDVI, with a mean difference in NDVI of 0.088 and seven days between high and low snow persistence pixels. These effects were stronger in NASA HLSS30 data, representative of Landsat data commonly used in greening analyses. Our findings indicate that unaccounted changes in fine-scale snow persistence may contribute to Arctic spectral greening and browning trends through either ecological responses of vegetation to snow cover or abiotic interactions between snow and the estimated peak NDVI. In order to improve our understanding of Arctic land-surface change, studies should integrate very-high-resolution data to estimate the dynamics of late season snow within coarser satellite pixels.

Introduction

Arctic temperatures are rising four times faster than those at lower latitudes (Rantanen *et al.*, 2022), driving concurrent changes in Arctic vegetation (Myers-Smith *et al.*, 2020) and snow cover (AMAP, 2017; Callaghan *et al.*, 2011). Earth observation provides a multidecadal basis for monitoring changes in the Arctic land-surface (AMAP, 2017). Since the 1980s, trends in the normalised difference vegetation index (NDVI) over the Arctic indicate both spectral greening (positive trends) over large areas (13% to 42%) and browning (negative trends) over more limited areas (1% to 4%), with remaining areas not experiencing a directional change (Myers-Smith *et al.*, 2020). Most commonly, greening is interpreted as enhanced vegetation productivity driven by warming temperatures (Myers-Smith *et al.*, 2020), while hypothesised drivers of browning are more diverse (Phoenix and Bjerke, 2016). However, the mid-to-coarse spatial resolutions of long-term satellite imagery (Landsat: 30 m; MODIS: 500 m; AVHRR GIMMS$_{3g}$: 8 km) used in greening analyses integrate both biotic and abiotic phenomena within the vegetation index of any given pixel (Myers-Smith *et al.*, 2020). Where the duration and extent of fine-resolution summer snow patches are changing, this may confound greening analyses (Myers-Smith *et al.*, 2020; Huemmrich *et al.*, 2021). To fully understand the drivers of Arctic spectral trends and their implications for both Arctic ecosystems and global climate feedbacks (Post *et al.*, 2019), we must quantify the influence of changing snow cover on these trends.

Arctic greening analyses integrate information across satellite pixels that do not match the spatial heterogeneity of the tundra land surface. Variation in vegetation biomass, species composition and non-vegetative land surfaces are found within the extents of satellite pixels (Beamish *et al.*, 2020; Myers-Smith *et al.*, 2020; Niittynen *et al.*, 2020; Suvanto, Le roux and Luoto, 2014). Remote sensing using drones gathers very-high-resolution imagery. At one Arctic site, spatial variation in NDVI was found to peak at 0.5 m (Assmann *et al.*, 2020). Fine-scale spatial variation results in spectral mixing, where abiotic phenomena are integrated within the spectral signature of satellite pixels (Pettorelli *et al.*, 2005; Beamish *et al.*, 2020; Myers-Smith *et al.*, 2020). Where abiotic phenomena and vegetation are both present within a satellite pixel, it is difficult to quantify their relative contribution to the pixel's NDVI (Pettorelli *et al.*, 2005).

Adding further complexity, greening analyses subsequently integrate NDVI observations across time. Studies interpolate seasonal NDVI curves per-pixel and take the curve's annual maximum value (*peak NDVI*), or less commonly sum the daily NDVI values above a given threshold (*time-integrated NDVI,* or *TI-NDVI*) (Bhatt *et al.*, 2021; Pettorelli *et al.*, 2005). Greening analyses assume these NDVI metrics represent the emergent seasonal vegetative signal of the area within a given pixel (Myers-Smith *et al.*, 2020; Pettorelli *et al.*, 2005). Both TI-NDVI and peak NDVI magnitude are used to infer vegetation productivity (e.g. Berner *et al.*, 2020; Bhatt *et al.*, 2013), while phenology is inferred from the timing of peak NDVI (e.g., May *et al.*, 2020). However, the integration of non-vegetative land surfaces within NDVI metrics may contribute to, or drive, trends in both the magnitude and timing of the peak NDVI. For this reason, the spectral dynamics of non-vegetative land-surfaces should be considered in Arctic greening analyses.

Snow cover is a dynamic non-vegetative land surface, which can influence the NDVI of a pixel both directly through spectral integration and indirectly through interactions with vegetation (Wang, Springer and Gamon, 2023; Pedersen *et al.*, 2018). Decreases in NDVI have been linked to spectral mixing of snow cover within experimental boreal plots (Wang, Springer and Gamon, 2023), with similar effects hypothesised for tundra landscapes (Beamish *et al.*, 2020; Myers-Smith *et al.*, 2020). Snow cover can also alter functional diversity (Niittynen, Heikkinen and Luoto, 2020), affect species distribution (Niittynen and Luoto, 2018) and is associated with lower biodiversity (Niittynen, Heikkinen and Luoto, 2018), while vegetation can in turn influence snow depth (Myers-Smith and Hik, 2013). Despite snow interacting with NDVI, greening analyses have been limited in their ability to account for snow by the spatial resolution of satellite imagery and snow data products (Beamish *et al.*, 2020). Some greening studies include coarse snow metrics (Zeng and Jia, 2013; Pedersen *et al.*, 2018), while others attempt to mask snow from analyses (e.g., Jia, Epstein and Walker, 2009; Berner *et al.*, 2020). Due to the imperfect classification of fine-scale snow cover within satellite data products (Stillinger *et al.*, 2023), snow is implicitly included in analyses even where studies have attempted to exclude it. Recent efforts to map fine-resolution snow cover at landscape scales with drone imagery (Rauhala *et al.*, 2023; Revuelto *et al.*, 2021) provide a solution for quantifying the influence of snow on NDVI metrics at Arctic focal sites.

In this study, we use drone imagery to test whether snow persistence within Sentinel-2 and NASA HLSS30 pixels is related to the timing and magnitude of peak NDVI at three tundra plots (Figure 1). We hypothesise greater snow persistence within satellite pixels will both limit the magnitude and delay the timing of peak NDVI, through either spectral integration of snow within NDVI observations or snow-vegetation interactions. Specifically, we ask: (1) Do satellite pixels with higher snow persistence have a lower magnitude peak NDVI? And (2), do satellite pixels with higher snow persistence have later timing of peak NDVI? To address these questions, we used drone repeat surveys to estimate within-pixel snow persistence across late spring and early summer for Sentinel-2 and HLSS30 data. We then extracted pixel-by-pixel peak NDVI magnitude and its timing from Sentinel-2 and HLSS30 products by fitting smooth-spline curves and interpolating across the growing season. Finally, we tested the relationship between snow persistence and both peak NDVI magnitude and timing using frequentist ordinary least squares (OLS) and Bayesian Integrated Nested Laplace Approximation (INLA). Overall, our study quantitatively assesses the influence of fine-scale snow persistence on two key vegetation metrics used in Arctic greening analyses.

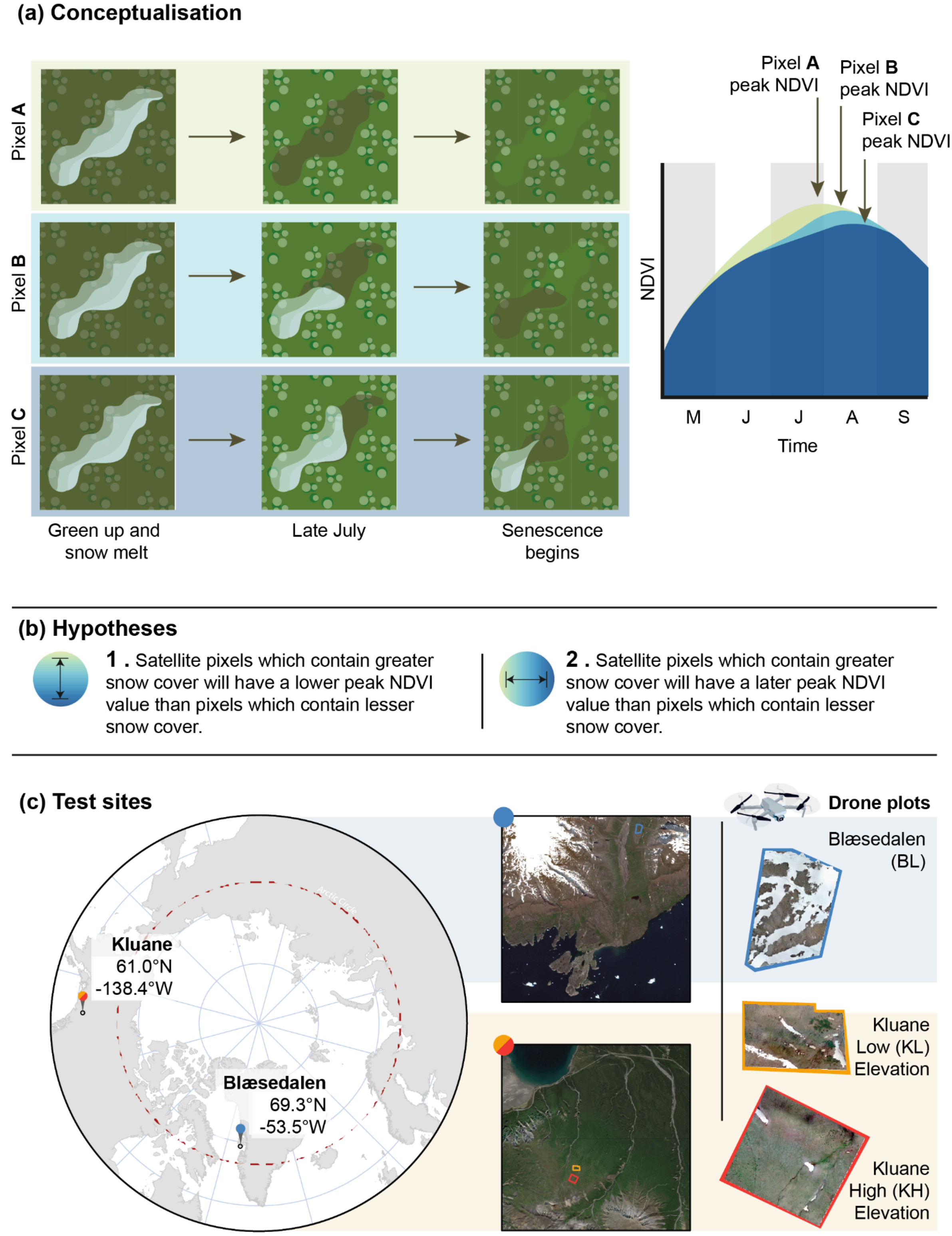

Figure 1. (a) Conceptual diagram of the project illustrating that pixels containing snow patches which persist later into the growing season will have seasonal NDVI curves of a different shape than pixels which contain lower snow persistence. (b) Hypotheses for this work, drawn from the differing conceptual NDVI curves. (c) Location of test plots within the Arctic/sub-Arctic, within their local context, and the drone plots themselves (1:15,000 scale).

Methods

Site Description

We tested the relationship between snow persistence and peak NDVI at one Arctic tundra (Blæsedalen: 69.3° N, 53.46° W) and one sub-Arctic alpine tundra field site (Kluane: 60.96° N, 138.42° W) (Figure 1). Blæsedalen is a north-south oriented glacial valley on the island of Qeqertarsuaq (Disko Island) in West Greenland and Kluane is a north-facing slope located within the foothills of the St. Elias range in the Yukon territory of northwest Canada. The 2000 - 2020 average annual precipitation was 480 mm at Blæsedalen and 304 mm at Kluane, of which ~36% and ~24% respectively fell between the months of November and February (Harris *et al.*, 2020).

At Blæsedalen, we chose a nine hectare plot (BL) on the valley's western aspect approximately 200 m above sea level, containing mesic tundra heath interspersed with bare and patterned ground. At Kluane, we chose two plots on a northern aspect. The lower plot (KL) was 7.1 hectares in size and 1620 m above sea level in an area of graminoid vegetation interspersed with tall shrubs, while the higher plot (KH) was 12.7 hectares in size and 1750 m above sea level in an area dominated by graminoid species. We chose plot locations to encompass late lying snow and vegetation typical of the surrounding landscape.

Satellite imagery acquisition and processing

Satellite imagery time-series were collated for two sensors: (1) the Multi-Spectral-Instrument (MSI) aboard the Sentinel-2 constellation; (2) the NASA Harmonised-Landsat-Sentinel S30 (HLSS30) product, analogous to the Optical-Land-Imager aboard Landsat 8 (Claverie *et al.*, 2018). As HLSS30 data is generated from Sentinel-2 imagery it reduced the impact on our analyses of differences in observation dates between sensors.

Sentinel-2 MSI Level-2A data were obtained through the Copernicus Browser by filtering for all imagery between April 1st and October 31st in the year of drone data collection (Kluane: 2022; Blæsedalen: 2023), then selecting all tiles visually free of cloud in proximity to the plots. This resulted in a time series of 16 images for Blæsedalen and 12 images for Kluane between the months of April and October (Tables S1, S2).

We used NASA EarthData Search to download all HLSS30 tiles matching the Sentinel-2 time series we generated for Blæsedalen. We did not generate time series of HLSS30 imagery for Kluane, as snow cover was too sparse to support meaningful analyses at a 30 m resolution. HLSS30 data was not available for October 17th and we identified quality issues with imagery from September (see supplementary 1.5.2, Figure S6), resulting in a time-series of 11 images for Blæsedalen (Table S3).

All satellite imagery was cropped to the extent of the drone imagery over each plot. All data handling was done with the terra package in R (version 1.7.55).

Drone imagery acquisition and processing

We derived snow cover from time-series of high resolution (5 cm) RGB imagery, which we captured through repeat drone surveys during the period of snow-melt and vegetation green-up at each plot (see supplementary 1.3). We processed all data through Agisoft Metashape v1.7.5 (St Petersburg, Russia) with flexible solving between bands to correct for band coregistration (Garieri *et al.*, 2022). From Agisoft Metashape we output a series of multiband geoTIFF files at a standardised spatial extent and grain size (5 cm), in the same coordinate reference system as the satellite imagery (Blæsedalen: UTM 21 N; Kluane: UTM 08 N).

Calculation of snow persistence metric

To calculate a metric describing the persistence of snow within Sentinel-2 and HLSS30 pixels, we first classified all drone pixels for every time step at each plot as snow-covered or snow-free using a simple threshold approach on the red-band (see supplementary S1.4). For each drone timestep at each plot, we extracted the number of snow-covered drone pixels within each satellite pixel (Sentinel-2, HLSS30) and calculated snow-cover-extent as a percentage of the satellite pixel area. We then plotted snow-cover-extent across time between the first and last drone image over each plot, interpolated linearly between the observations and integrated the area under the curve (Figure 3d). The resulting snow persistence metric provides a combined measure of snow cover extent and duration per satellite pixel. However, different drone observation dates (Figure 4d) at each plot mean the snow persistence metric is plot-specific and subsequent analyses must treat plots separately.

Calculation of peak NDVI

To extract the timing and magnitude of peak NDVI from satellite pixels, we derived an NDVI time series for each plot by calculating the standardised difference between the red and near-infrared band of Sentinel-2 and HLSS30 imagery (see supplementary 1.5). We removed noise outside the growing season by re-assigning negative NDVI observations a value of zero (Beck *et al.*, 2006). To ensure curve fitting was equally bounded by low NDVI in the spring and autumn, we added three synthetic NDVI observations of zero to the end of each time series (see supplementary 1.5). We then fitted both double-logistic curves (Beck *et al.*, 2006) and smooth-spline curves (Berner *et al.*, 2020) to the NDVI time-series. For all plots and sensors, we found smooth-spline curves best represented our data (Figures S11-13) and extracted the peak NDVI value and its timing for each pixel.

Statistical analyses

To compare high and low snow persistence Sentinel-2 pixels, we calculated the difference between the average magnitude and timing of peak NDVI for pixels in the upper and lower quartile of snow persistence at each plot. We then averaged the difference across all plots. We subsequently used linear models to test whether peak NDVI magnitude and timing are related to snow persistence within Sentinel-2 and HLSS30 pixels. As the snow persistence metric is plot-specific, we developed separate models for peak NDVI timing and magnitude at each plot and for each satellite data product.

First, we tested the relationships between peak NDVI magnitude and timing with snow persistence using ordinary least squares (OLS) regression. For Blæsedalen and Kluane Low, simple linear models provided a sufficient fit to the data. However, visual inspection of the Kluane High data indicated a non-linear relationship and we fitted logarithmic models for this plot instead ($y = ln(x+1)$, where y is peak NDVI magnitude or timing and x is the snow persistence metric). The non-linearity of the relationships at Kluane High could be driven by the inflation of zero and near-zero values in the snow persistence predictor combined with a reduced variance in the response variables towards the higher end of the predictor (Figures S15, S16).

Next, we assessed whether spatial autocorrelation in the predictor and response variables influenced the observed relationships (see supplementary S1.6.1). We found significant spatial autocorrelation for all variables at all plots, with variogram range values between ~13-125 m. We then fitted all models again using Bayesian Integrated Nested Laplace Approximation (INLA) with a Matérn 2D covariance function (r/INLA, v24.02.09) to account for the observed spatial autocorrelation. When fitting these models, we followed the recommendations of Beguin *et al.* (2012; see supplementary S1.6.2).

Both the simple OLS and spatial INLA Matérn 2D regressions were consistent in the direction and significance of trends for all models, with the exception of Sentinel-2 peak NDVI magnitude at Blæsedalen. Here, the INLA Matérn 2D indicated non-linearities in the data after accounting for spatial autocorrelation. To address these concerns, we tested whether incorporating a breakpoint at the snow persistence value of five would provide a more meaningful fit.

Finally, at Blæsedalen we compared the effect size between each model using Sentinel-2 data and the equivalent model using HLSS30 data.

In the remainder of this manuscript we will use the OLS models for visualisation due to their simplicity and ease of interpretation. We refer to the INLA Matérn 2D models in the text and report full outputs of all models in the supplementary materials.

Results

Seasonal NDVI curves differ between high and low snow persistence Sentinel-2 pixels

We observed variance in the amplitude and timing of curves fitted to the NDVI time series for the Sentinel-2 pixels. Taken across all plots, those pixels with snow persistence values in the lower quartile had a peak NDVI that was on average 0.088 higher and 7.64 days earlier than for pixels in the upper quartile (Figure 2).

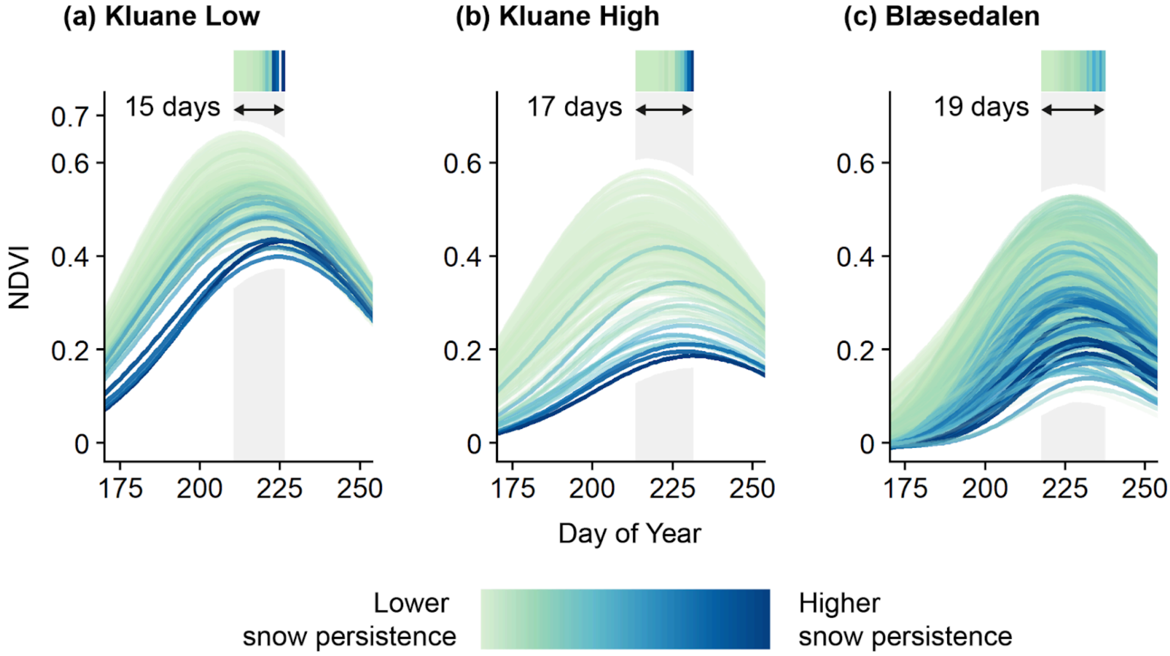

Figure 2. NDVI curves for Sentinel-2 pixels with higher snow persistence generally have a lower and later peak than curves for pixels with lower snow persistence. Curves plotted from NDVI values fitted by a smoothed-spline model based on observed Sentinel-2 NDVI across a single season. The shaded grey area represents the range of days within which all pixels at each site reached their peak NDVI, while the corresponding colour ribbon represents the mean snow persistence of all pixels which reached peak NDVI on each day within that period. The snow persistence colour gradient shows the relative snow persistence of that point standardised to the maximum and minimum snow persistence within each plot.

Higher snow persistence is associated with lower peak NDVI in Sentinel-2 data

A higher snow-persistence was associated with a lower peak NDVI in the Sentinel-2 pixels across all three plots (Figure 3). The OLS models using a linear fit showed significant ($p < 0.01$) negative relationships between snow persistence and peak NDVI magnitude at all plots (KL: -0.005 ± 0.001; KH: -0.023 ± 0.001; BL: -0.005 ± 0.001; Table S4). For Kluane High, the logarithmic model ($y \sim \ln(x + 1)$) also indicated a significant negative relationship (-0.089 ± 0.004, $p < 0.01$; Table S5). The INLA Matérn 2D models effectively accounted for spatial autocorrelation (Figures S20-23). The slope estimates for Kluane Low (mean = -0.003, 95%CI [-0.004, -0.002]) and Kluane High (mean = -0.005, 95%CI [-0.006, -0.004]) were both significantly negative. However, the 95%CI for Blæsedalen overlapped with zero (Table S16). Here, the breakpoint model indicated an initially positive slope (mean = 0.003, 95%CI [0.001, 0.005]) for the snow-persistence interval [0, 5], followed by a negative slope (mean = -0.002, 95%-CI [-0.004, -0.00031]) for the interval (5, 24] (Table S17).

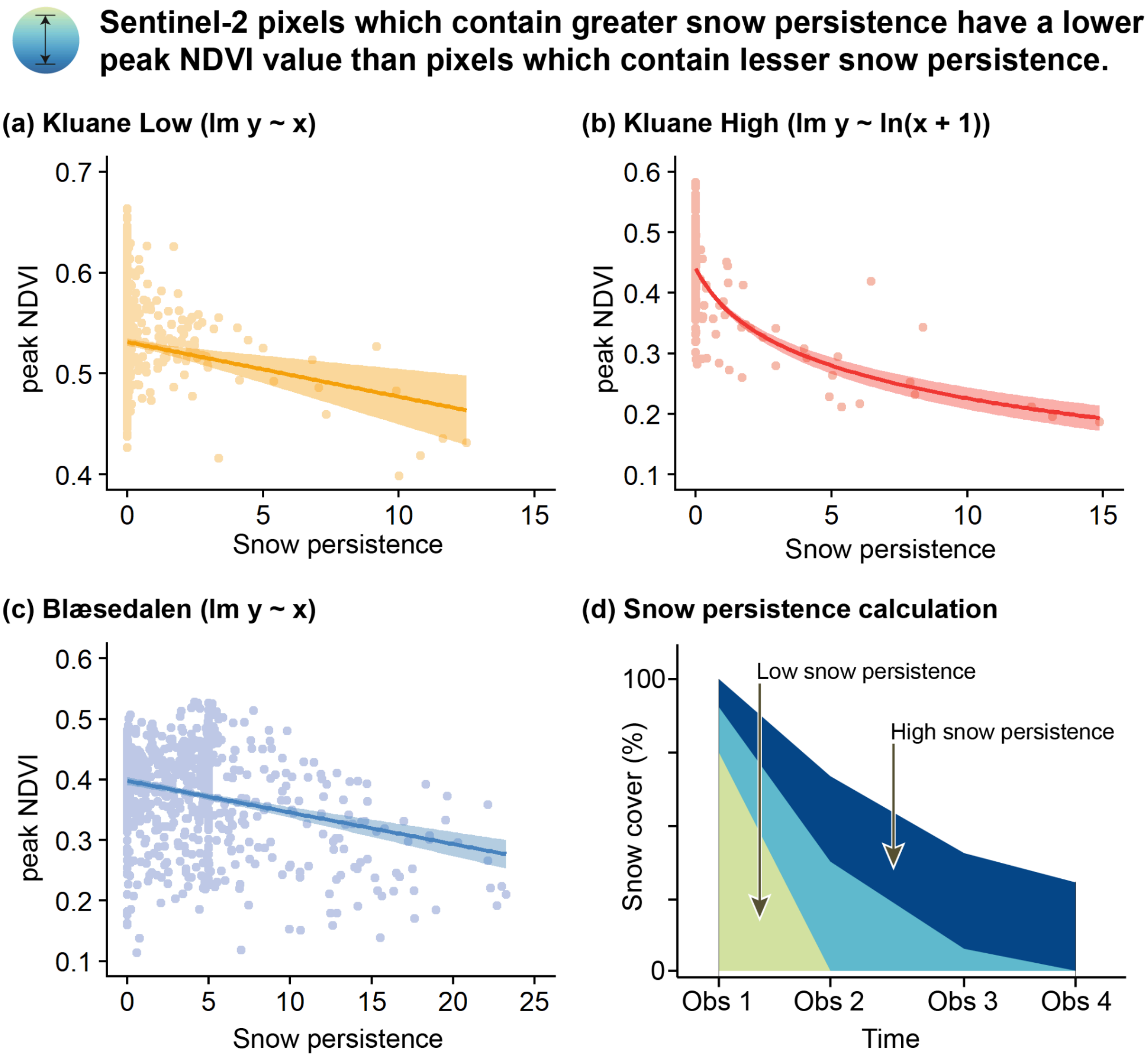

Figure 3. (a, b, c) Peak NDVI magnitude had a negative relationship with snow persistence in Sentinel-2 data at all three sites. Lines represent the predicted mean responses from the OLS regression. For Kluane Low (a) and Blæsedalen (c) these represent a linear fit (y ~ x). For Kluane High (b) the line represents a logarithmic fit (y ~ ln(x + 1)). (d) Conceptual diagram showing the calculation of snow persistence as the integrated snow cover between the first and last imagery date at a given site, interpolating linearly between observations.

Higher snow persistence is associated with later peak NDVI in Sentinel-2 data

A higher snow persistence was associated with later peak NDVI timing in Sentinel-2 pixels across all three plots (Figure 4). The OLS models using a linear fit showed significant (p < 0.01) positive relationships between snow persistence and peak NDVI timing at all plots (KL: 0.91 ± 0.054; KH: 1.392 ± 0.056; BL: 0.38 ± 0.022; Table S6). For Kluane High, the logarithmic model (y ~ ln(x + 1) (Figure 4b) showed a significant positive relationship (5.696 ± 0.185, p < 0.01; Table S7). INLA Matérn 2D models effectively accounted for spatial autocorrelation (Figures S25-27). The slope estimates for Kluane Low (mean = 0.458, 95%CI [0.38, 0.537]), Kluane High (mean = 0.57, 95%CI [0.489, 0.652]) and Blæsedalen (mean = 0.24, 95%CI [0.202, 0.277]) were all significantly positive (Table S18).

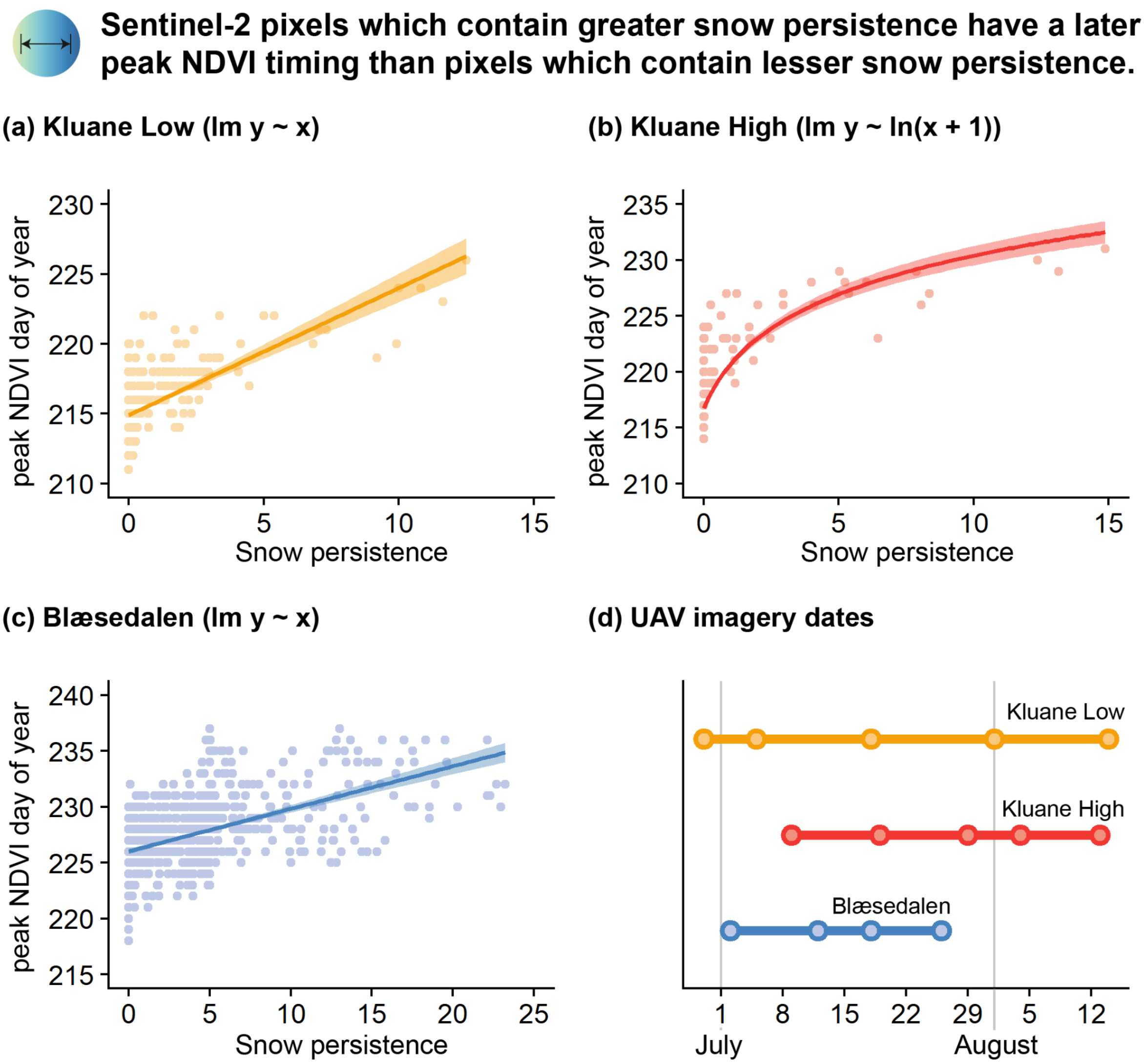

Figure 4. (a, b, c) Peak NDVI timing had a positive relationship with snow persistence in Sentinel-2 data at all three sites. Lines for Kluane Low (a) and Blæsedalen (c) were fitted using a linear fit. The line for Kluane High (b) was fitted using a logarithmic model (y ~ ln(x + 1). (d) Dates of drone imagery used to generate snow persistence metric. Differences in timing of observations between sites means a universal metric could not be calculated.

Higher snow persistence predicts peak NDVI value and timing in NASA HLSS30 data

A higher snow persistence was associated with both a lower peak NDVI magnitude and later peak NDVI timing in HLSS30 data at Blæsedalen (Figure 5). The simple OLS models found a negative relationship between snow persistence and peak NDVI magnitude (-0.01, $p < 0.01$; Table S4) and a positive relationship between snow persistence and peak NDVI timing (1.399 ± 0.126, $p < 0.01$; Table S6). INLA Matérn 2D models effectively accounted for spatial autocorrelation (Figures S24, S28). The 95% CI of the posterior distribution indicated a negative slope between snow persistence and peak NDVI magnitude (mean = -0.01, 95%CI: [-0.013, -0.006], Table S16), and a positive slope between snow persistence and peak NDVI timing (mean = 1.385, 95%CI [1.138, 1.632]; Table S18). We found that for HLSS30 data the effect sizes between snow persistence and peak NDVI metrics are stronger than in Sentinel-2 data.

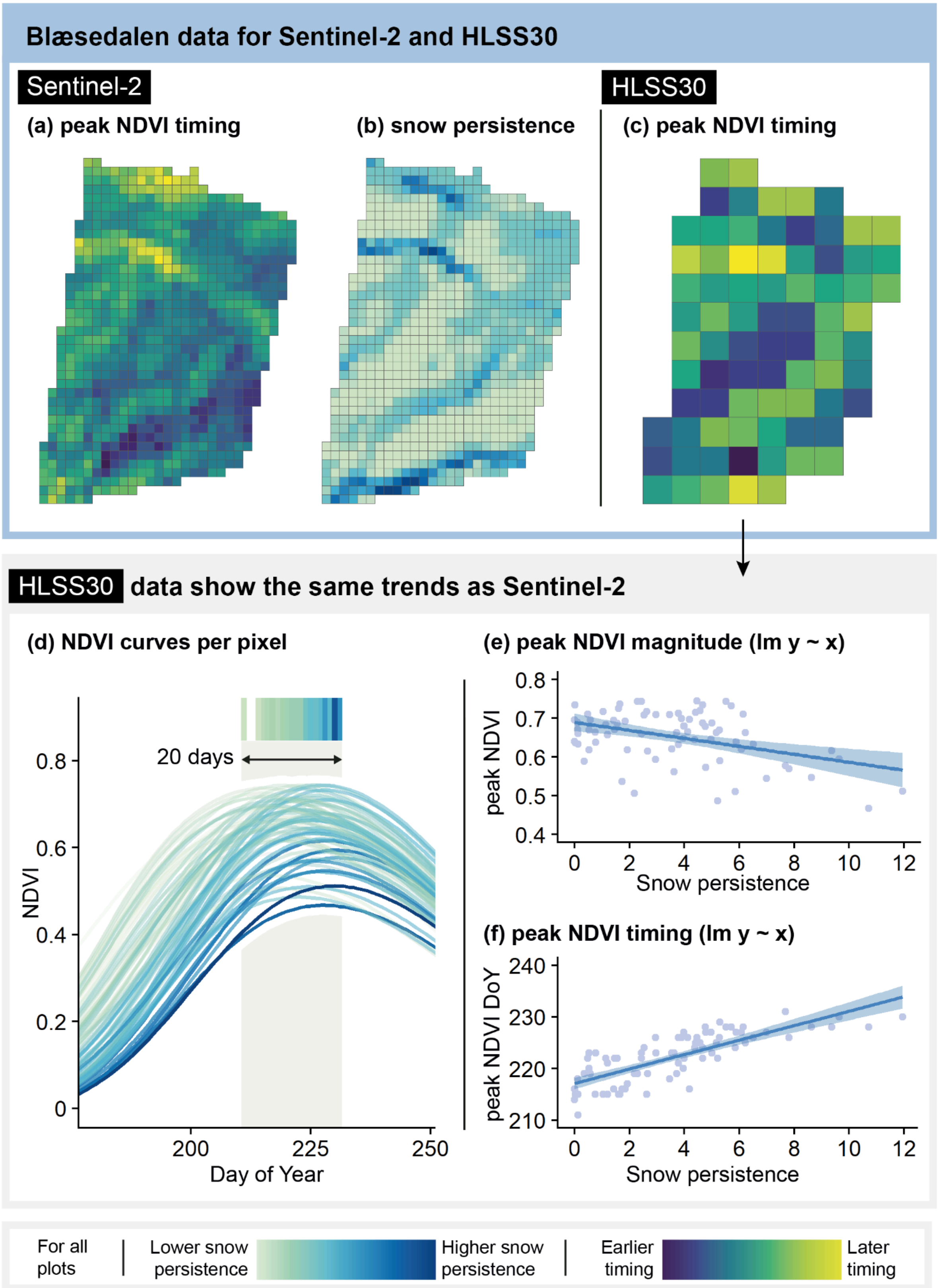

Figure 5. Snow persistence was related to the magnitude and timing of peak NDVI in HLSS30 data at Blæsedalen. The relationships were consistent with those found in Sentinel-2 data, but the effect sizes were stronger. Mapped Sentinel-2 peak NDVI timing (a) visually corresponds with snow persistence (b) and this spatial patterning is preserved in HLSS30 peak NDVI timing (c). The shape and distribution of NDVI curves was similar between coarser HLSS30 data (d) and finer Sentinel-2 data (Figure 1c). (e) HLSS30 peak NDVI magnitude had a relationship with snow persistence which is consistent with Sentinel-2 data (Figure 3c). (f) HLSS30 peak NDVI timing had a relationship with snow persistence which is consistent with Sentinel-2 data (Figure 4c). The snow persistence colour gradient shows the relative snow persistence of that point standardised to the maximum and minimum snow persistence for each data product (Sentinel-2, HLSS30) at the Blæsedalen plot. The peak NDVI timing colour gradient shows the relative peak NDVI timing of that point standardised to the maximum and minimum peak NDVI day of year for each data product at the Blæsedalen plot.

Discussion

Summary

Our analyses show that higher snow persistence within satellite pixels corresponds with a lower magnitude and delayed timing of peak NDVI across two tundra sites and two satellite data products at different spatial and spectral resolutions. We found only one exception, when accounting for spatial autocorrelation at Blæsedalen, where initial increases in snow persistence corresponded with a *higher* magnitude of peak NDVI. Surprisingly, we found relationships between snow persistence and peak NDVI were stronger in coarser HLSS30 data than in Sentinel-2 data. Our findings indicate that snow persistence contributes to spatial variability in the timing and magnitude of peak NDVI in satellite data products. Changes in sub-pixel snow persistence are poorly accounted for in analyses of Arctic greening (Myers-Smith *et al.*, 2020), yet we provide initial evidence that they may in places contribute to or drive observed Arctic greening and browning trends.

Ecological interactions between snow and peak NDVI magnitude

Reduced vegetation productivity or different species composition in areas of consistently late-lying snow patches may explain the observed correspondence between higher snow persistence and lower magnitude of peak NDVI. Limited vegetation productivity due to a snow-shortened growing season has previously been proposed to explain negative relationships between coarse snow products, peak NDVI magnitude (Tassone *et al.*, 2024; Crichton *et al.*, 2022; Wang *et al.*, 2018) and early season NDVI (Bjerke *et al.*, 2015). Snow is also a driver of species distribution (Niittynen and Luoto, 2018) and differences in NDVI have previously been attributed to community composition (e.g., Jia, Epstein and Walker, 2004). As we did not incorporate plot-level vegetation data in this analysis, we are unable to partition these effects or estimate the influence of snow-driven differences in productivity and species composition on NDVI across the growing season. Nonetheless our results indicate that either, or both, of these mechanisms could be present.

Reversal of snow - NDVI relationships at low snow persistence values

At Blæsedalen we found the relationship between higher snow persistence and lower peak NDVI magnitude is reversed at low snow persistence values, where peak NDVI magnitude initially increases with snow persistence. Similar results have been reported for MODIS (Pedersen *et al.*, 2018) and AVHRR GIMMS$_{g3}$ data (Wang *et al.*, 2018), where limited increases in snow cover provide greater access to moisture without restricting access to other resources. Other possible explanations include insulation of the soil from ground frost (Bjerke *et al.*, 2015) and of roots from frost injury (Templer, 2012). Changes in the direction of the relationship between snow persistence and peak NDVI magnitude may exist for all our plots, however our data do not capture variation in snow persistence where snow completely melted out before the first drone observation. Where relationships with changes of direction exist, these would complicate our ability to predict vegetative and spectral responses to changing Arctic snow cover (AMAP, 2017).

Ecological interactions between snow and peak NDVI timing

We found that higher snow persistence was associated with a later timing of peak NDVI in Sentinel-2 and HLSS30 data. Similarly, many studies have found that high pre-melt snow water equivalent or late snowmelt timing delays NDVI derived spring phenology metrics due to late phenological cues and resource access (Qi *et al.,* 2021; Assmann *et al.*, 2019; Bieniek *et al.,* 2015; Zeng and Jia, 2013; Zeng, Jia and Epstein, 2011), with these relationships supported by field studies (e.g., Bjorkman *et al.,* 2015). However, Pedersen et al. (2018) found a non-linear relationship in MODIS (500 m) data where both early and late snowmelt timing resulted in an earlier peak of NDVI. We suggest that non-linear relationships between snow and phenology may be a function of phenological mixing within coarser satellite pixels (Helman, 2018). The linear relationship that we found between higher snow persistence and later timing of peak NDVI has precedent in both NDVI derived spring phenology metrics and ecological field studies.

Abiotic interactions between snow and peak NDVI

While correspondence between snow persistence and peak NDVI may represent ecological responses of vegetation to late lying snow, it may alternatively represent abiotic spectral mixing of snow within a satellite pixel's NDVI. Fractional snow cover decreases NDVI (Wang, Springer and Gamon, 2023) and it follows that snow coincident with the timing of peak NDVI would limit peak NDVI magnitude. However, this effect is limited for our data as no pixels at Kluane and few pixels at Blæsedalen (Sentinel-2: 7.25%; Landsat: 25.64%) contain snow beyond July 26th. Instead, we found an indirect effect, whereby late-lying snow melts rapidly and produces an outsized NDVI response (Huemmrich *et al.*, 2021), which is poorly represented by curve fitting models and results in underestimated magnitude of peak NDVI (Figure S14). Similarly, the response of NDVI to late-season snow melt may in places drive the timing of peak NDVI more than vegetation phenology, as reported for spring phenology metrics (Jin *et al.*, 2017). Most studies assume NDVI represents vegetation productivity, yet the NDVI and consequently the timing and magnitude of peak NDVI may be mechanistically influenced by fine-scale snow cover, with similar effects likely for aggregate metrics such as the TI-NDVI.

Snow - peak NDVI relationships across spatial and spectral resolutions

Despite a spatial resolution nine times coarser than Sentinel-2, relationships between snow and both the magnitude and timing of peak NDVI were stronger in HLSS30 data. It is possible that the signal-to-noise ratio is stronger in HLSS30 data or that the spectral integration of snow cover is stronger in NDVI derived from HLSS30 data. Variation in the strength of relationships between snow and peak NDVI magnitude dependent on the spatial and spectral resolution of data contributes one possible explanation to observed differences in NDVI trends between satellite data products (Myers-Smith *et al.*, 2020). Regardless of mechanism, we found a strong association of snow persistence with the timing and magnitude of peak NDVI in HLSS30 data, which represent the spatial and spectral resolution of Landsat data commonly used (Myers-Smith *et al.*, 2020) in Arctic greening analyses.

Implications for Arctic greening analyses

Changes in snow cover have been observed across the Arctic (AMAP, 2017) and our findings indicate that reductions in late-lying snow cover may induce spectral *greening*, whereas increased snow cover could induce spectral *browning*. While this effect may represent ecological responses to snow cover, we suggest that the spectral integration of changing snow within satellite pixels may in places abiotically drive both the magnitude and timing of peak NDVI. Where snow drives spectral trends, there is greater potential for misinterpreting vegetation indices as true changes in vegetation productivity or phenology. Underestimates of peak NDVI magnitude due to the presence of snow may lead to the omission of areas of genuine vegetation change. However, our analyses were limited to a single season and by spatially autocorrelated plots of limited extents, whereby simple OLS models may overestimate and INLA Matérn 2D models may underestimate effect sizes (Beguin *et al.*, 2012). Future research could use multi-season very-high-resolution satellite imagery to relate snow persistence within Landsat and MODIS pixels to spectral trends over time, incorporating plot level vegetation data wherever possible.

Conclusions

Spectral analyses of satellite data products show that the Arctic is ‘*greening*’ in many locations and ‘*browning*’ in others, with these trends commonly attributed to temperature driven changes in Arctic vegetation. However, recent work has highlighted the complexity of heterogeneous greening trends (Myers-Smith *et al.*, 2020). Snow cover has changed in many Arctic locations (AMAP, 2017), yet late season snow is often too fine in scale to be either accounted for or masked from mid-to-coarse spatial resolution satellite data products. We demonstrate that this fine-scale snow persistence within satellite pixels is associated with both a lower magnitude and later timing of peak NDVI, with stronger effect sizes for HLSS30 data. Where snow cover is changing, it may drive spectral greening and browning trends through either ecological responses of vegetation or abiotic integration of snow cover within the estimated peak NDVI. We recommend that future work explores the spatial extent of the relationship between snow and peak NDVI and better resolves the mechanisms underlying these relationships.

Data availability statement

The data and code that support the findings of this study are openly available at the following URL/DOI: https://github.com/calumhoad/snowpersistence/tree/main

Acknowledgements

We would like to thank everyone who helped with field data collection in the Canadian Yukon during 2022 and in Greenland during 2023, including Joseph Everest, Erica Zaja, Jiri Subrt, Sian Williams and Mariana García Criado. For help with drones and sensors, particular thanks go to Tom Wade at the University of Edinburgh Airborne Research and Innovation facility, and Alex Merrington, Jack Gillespie, Craig Atkins and Robbie Ramsay at the NERC Field Spectroscopy Facility. Additional thanks to Alan Hobbs, Colin Kay and Graham Mitchell from the NERC Geophysical Equipment Facility.

We thank Tim Gyger for support and consultation on our statistical methods, Gwenn Flowers for the time taken to provide climate data for Kluane and Kirsten Schmidt-Pedersen for sharing her extensive knowledge of the people, plants and animals of Qeqertarsuaq, Greenland.

Funding for this research was provided by NERC through a SENSE CDT studentship (NE/T00939X/1), Tundra Time (NE/W006448/1), a 2023 UK-Greenland Arctic Bursary, a Geophysical Equipment Facility loan (1152), and a Field Spectroscopy Facility loan (891.0111). Additional funding was provided by a Scottish Alliance for GeoScience, Environment and Society (SAGES) small grant scheme award to Calum Hoad.

We thank Kluane First Nation and Champagne and Aishihik First Nations for their permission to work on their lands. We gratefully acknowledge the people of Kalaallit Nunaat in general, and of Qeqertarsuaq in particular, for being able to conduct this research on their land. We thank Outpost Research Station and Arctic Station for logistical support.

Author Contributions

Calum G. Hoad: Conceptualisation (lead); Data curation (lead); Formal analysis (equal); Funding acquisition (equal); Investigation (lead); Methodology (lead); Project administration (lead); Resources (lead); Software (equal); Visualisation (lead); Writing – original draft (lead); Writing – review and editing (lead). **Isla H. Myers-Smith:** Conceptualisation (supporting); Formal analysis (supporting); Funding acquisition (equal); Methodology (supporting); Resources (supporting); Supervision (lead); Visualisation (supporting); Writing – review and editing (equal). **Jeff T. Kerby:** Conceptualisation (supporting); Methodology (supporting); Supervision (equal); Visualisation (supporting); Writing – review and editing (equal). **Claudia Colesie:** Conceptualisation (supporting); Funding acquisition (supporting); Supervision (equal); Project administration (supporting); Resources (supporting); Visualisation (supporting); Writing – review and editing (equal). **Jakob J. Assmann:** Conceptualisation (supporting); Data curation (supporting); Formal analysis (equal); Investigation (supporting); Methodology (supporting); Supervision (lead); Software (equal); Visualisation (supporting); Writing – original draft (supporting); Writing – review and editing (equal).

References

AMAP (2017) *Snow, Water, Ice and Permafrost in the Arctic (SWIPA) 2017*. Oslo, Norway, p. xiv + 269. Available at: https://www.amap.no/documents/doc/snow-water-ice-and-permafrost-in-the-arctic-swipa-2017/1610.

Assmann, J.J. *et al.* (2019) 'Local snow melt and temperature—but not regional sea ice—explain variation in spring phenology in coastal Arctic tundra', *Global Change Biology*, 25(7), pp. 2258–2274. Available at: https://doi.org/10.1111/gcb.14639.

Assmann, J.J. *et al.* (2020) 'Drone data reveal heterogeneity in tundra greenness and phenology not captured by satellites', *Environmental Research Letters*, 15(12). Available at: https://doi.org/10.1088/1748-9326/abbf7d.

Beamish, A. *et al.* (2020) 'Recent trends and remaining challenges for optical remote sensing of Arctic tundra vegetation: A review and outlook', *Remote Sensing of Environment*, 246(May), p. 111872. Available at: https://doi.org/10.1016/j.rse.2020.111872.

Beck, P.S.A. *et al.* (2006) 'Improved monitoring of vegetation dynamics at very high latitudes: A new method using MODIS NDVI', *Remote Sensing of Environment*, 100(3), pp. 321–334. Available at: https://doi.org/10.1016/j.rse.2005.10.021.

Beguin, J. *et al.* (2012) 'Hierarchical analysis of spatially autocorrelated ecological data using integrated nested Laplace approximation', *Methods in Ecology and Evolution*, 3(5), pp. 921–929. Available at: https://doi.org/10.1111/j.2041-210X.2012.00211.x.

Berner, L.T. *et al.* (2020) 'Summer warming explains widespread but not uniform greening in the Arctic tundra biome', *Nature Communications*, 11(1), pp. 1–12. Available at: https://doi.org/10.1038/s41467-020-18479-5.

Bhatt, U.S. *et al.* (2013) 'Recent declines in warming and vegetation greening trends over pan-arctic tundra', *Remote Sensing*, 5(9), pp. 4229–4254. Available at: https://doi.org/10.3390/rs5094229.

Bhatt, U.S. et al. (2021) 'Climate drivers of Arctic tundra variability and change using an indicators framework', *Environmental Research Letters*, 16(5), p. 055019. Available at: https://doi.org/10.1088/1748-9326/abe676.

Bieniek, P.A. *et al.* (2015) 'Climate Drivers Linked to Changing Seasonality of Alaska Coastal Tundra Vegetation Productivity', *Earth Interactions*, 19(19), pp. 1–29. Available at: https://doi.org/10.1175/EI-D-15-0013.1.

Bjerke, J.W. *et al.* (2015) 'Impacts of snow season on ground-ice accumulation, soil frost and primary productivity in a grassland of sub-Arctic Norway', *Environmental Research Letters*, 10(9), p. 095007. Available at: https://doi.org/10.1088/1748-9326/10/9/095007.

Bjorkman, A.D. *et al.* (2015) 'Contrasting effects of warming and increased snowfall on Arctic tundra plant phenology over the past two decades', *Global Change Biology*, 21(12), pp. 4651–4661. Available at: https://doi.org/10.1111/gcb.13051.

Callaghan, T.V. *et al.* (2011) 'The changing face of arctic snow cover: A synthesis of observed and projected changes', *Ambio*, 40(SUPPL. 1), pp. 17–31. Available at: https://doi.org/10.1007/s13280-011-0212-y.

Claverie, M. *et al.* (2018) 'The Harmonized Landsat and Sentinel-2 surface reflectance data set', *Remote Sensing of Environment*, 219, pp. 145–161. Available at:

https://doi.org/10.1016/j.rse.2018.09.002.

Crichton, K.A. *et al.* (2022) ‘Seasonal climate drivers of peak NDVI in a series of Arctic peatlands’, *Science of The Total Environment*, 838, p. 156419. Available at: https://doi.org/10.1016/j.scitotenv.2022.156419.

Garieri, P. *et al.* (2022) ‘Multi-camera geometric calibration: pre-calibration and on-the-job calibration of the MAIA multispectral system’, in *The International Archives of the Photogrammetry, Remote Sensing and Spatial Information Sciences*. *XXIV ISPRS Congress (2022 edition)*, Nice, France, pp. 665–672. Available at: https://doi.org/10.5194/isprs-archives-XLIII-B2-2022-665-2022.

Helman, D. (2018) ‘Land surface phenology: What do we really “see” from space?’, *Science of The Total Environment*, 618, pp. 665–673. Available at: https://doi.org/10.1016/j.scitotenv.2017.07.237.

Hijmans, R.J. (2023) ‘terra: Spatial Data Analysis’. (R package). Available at: https://CRAN.R-project.org/package=terra.

Huemmrich, K.F. *et al.* (2021) ‘Canopy reflectance models illustrate varying NDVI responses to change in high latitude ecosystems’, *Ecological Applications*, 31(8), p. e02435. Available at: https://doi.org/10.1002/eap.2435.

Jia, G.J., Epstein, H.E. and Walker, D.A. (2004) ‘Controls over intra-seasonal dynamics of AVHRR NDVI for the Arctic tundra in northern Alaska’, *International Journal of Remote Sensing*, 25(9), pp. 1547–1564. Available at: https://doi.org/10.1080/0143116021000023925.

Jia, G.J., Epstein, H.E. and Walker, D.A. (2009) ‘Vegetation greening in the canadian arctic related to decadal warming’, *Journal of Environmental Monitoring*, 11(12), pp. 2231–2238. Available at: https://doi.org/10.1039/b911677j.

Jin, H. *et al.* (2017) ‘Disentangling remotely-sensed plant phenology and snow seasonality at northern Europe using MODIS and the plant phenology index’, *Remote Sensing of Environment*, 198, pp. 203–212. Available at: https://doi.org/10.1016/j.rse.2017.06.015.

May, J.L. *et al.* (2020) ‘NDVI Changes Show Warming Increases the Length of the Green Season at Tundra Communities in Northern Alaska: A Fine-Scale Analysis’, *Frontiers in Plant Science*, 11. Available at: https://doi.org/10.3389/fpls.2020.01174.

Myers-Smith, I.H. *et al.* (2020) ‘Complexity revealed in the greening of the Arctic’, *Nature Climate Change*, 10(2), pp. 106–117. Available at: https://doi.org/10.1038/s41558-019-0688-1.

Myers-Smith, I.H. and Hik, D.S. (2013) ‘Shrub canopies influence soil temperatures but not nutrient dynamics: An experimental test of tundra snow-shrub interactions’, *Ecology and Evolution*, 3(11), pp. 3683–3700. Available at: https://doi.org/10.1002/ece3.710.

Niittynen, P. *et al.* (2020) ‘Fine-scale tundra vegetation patterns are strongly related to winter thermal conditions’, *Nature Climate Change*, 10(12), pp. 1143–1148. Available at: https://doi.org/10.1038/s41558-020-00916-4.

Niittynen, P., Heikkinen, R.K. and Luoto, M. (2018) ‘Snow cover is a neglected driver of Arctic biodiversity loss’, *Nature Climate Change*, 8(11), pp. 997–1001. Available at: https://doi.org/10.1038/s41558-018-0311-x.

Niittynen, P., Heikkinen, R.K. and Luoto, M. (2020) ‘Decreasing snow cover alters functional composition and diversity of Arctic tundra’, *Proceedings of the National Academy of Sciences*, 117(35), pp. 21480–21487. Available at: https://doi.org/10.1073/pnas.2001254117.

Niittynen, P. and Luoto, M. (2018) 'The importance of snow in species distribution models of arctic vegetation', *Ecography*, 41(6), pp. 1024–1037. Available at: https://doi.org/10.1111/ecog.03348.

Pedersen, S.H. *et al.* (2018) 'Quantifying snow controls on vegetation greenness', *Ecosphere*, 9(6). Available at: https://doi.org/10.1002/ecs2.2309.

Pettorelli, N. *et al.* (2005) 'Using the satellite-derived NDVI to assess ecological responses to environmental change', *Trends in Ecology and Evolution*, 20(9), pp. 503–510. Available at: https://doi.org/10.1016/j.tree.2005.05.011.

Phoenix, G.K. and Bjerke, J.W. (2016) 'Arctic browning: extreme events and trends reversing arctic greening', *Global Change Biology*, 22(9), pp. 2960–2962. Available at: https://doi.org/10.1111/gcb.13261.

Post, E. *et al.* (2019) 'The polar regions in a 2°C warmer world', *Science Advances*, 5(12). Available at: https://doi.org/10.1126/sciadv.aaw9883.

Qi, Y. *et al.* (2021) 'Relationship between vegetation phenology and snow cover changes during 2001–2018 in the Qilian Mountains', *Ecological Indicators*, 133, p. 108351. Available at: https://doi.org/10.1016/j.ecolind.2021.108351.

Rantanen, M. et al. (2022) 'The Arctic has warmed nearly four times faster than the globe since 1979', *Communications Earth & Environment*, 3(1), pp. 1–10. Available at: https://doi.org/10.1038/s43247-022-00498-3.

Rauhala, A. *et al.* (2023) 'Measuring the spatiotemporal variability in snow depth in subarctic environments using UASs – Part 1: Measurements, processing, and accuracy assessment', *The Cryosphere*, 17(10), pp. 4343–4362. Available at: https://doi.org/10.5194/tc-17-4343-2023.

Revuelto, J. *et al.* (2021) 'Intercomparison of UAV platforms for mapping snow depth distribution in complex alpine terrain', *Cold Regions Science and Technology*, 190, p. 103344. Available at: https://doi.org/10.1016/j.coldregions.2021.103344.

Rue, H., Martino, S. and Chopin, N. (2009) 'Approximate Bayesian Inference for Latent Gaussian Models by Using Integrated Nested Laplace Approximations', *Journal of the Royal Statistical Society*, *Series B*, 71, pp. 319–392. Available at: www.r-inla.org.

Stillinger, T. *et al.* (2023) 'Landsat, MODIS, and VIIRS snow cover mapping algorithm performance as validated by airborne lidar datasets', *The Cryosphere*, 17(2), pp. 567–590. Available at: https://doi.org/10.5194/tc-17-567-2023.

Suvanto, S., Le roux, P.C. and Luoto, M. (2014) 'Arctic-alpine vegetation biomass is driven by fine-scale abiotic heterogeneity', *Geografiska Annaler: Series A, Physical Geography*, 96(4), pp. 549–560. Available at: https://doi.org/10.1111/geoa.12050.

Tassone, M.S. *et al.* (2024) 'Drivers of heterogeneity in tundra vegetation productivity on the Yamal Peninsula, Siberia, Russia', *Environmental Research: Ecology*, 3(1), p. 015003. Available at: https://doi.org/10.1088/2752-664X/ad220f.

Templer, P.H. (2012) 'Changes in winter climate: soil frost, root injury, and fungal communities', *Plant and Soil*, 353(1), pp. 15–17. Available at: https://doi.org/10.1007/s11104-011-1064-8.

Wang, R., Springer, K.R. and Gamon, J.A. (2023) ‘Confounding effects of snow cover on remotely sensed vegetation indices of evergreen and deciduous trees: An experimental study’, *Global Change Biology*, 29(21), pp. 6120–6138. Available at: https://doi.org/10.1111/gcb.16916.

Wang, X. *et al.* (2018) ‘Disentangling the mechanisms behind winter snow impact on vegetation activity in northern ecosystems’, *Global Change Biology*, 24(4), pp. 1651–1662. Available at: https://doi.org/10.1111/gcb.13930.

Zeng, H. and Jia, G. (2013) ‘Impacts of snow cover on vegetation phenology in the arctic from satellite data’, *Advances in Atmospheric Sciences*, 30(5), pp. 1421–1432. Available at: https://doi.org/10.1007/s00376-012-2173-x.

Zeng, H., Jia, G. and Epstein, H. (2011) ‘Recent changes in phenology over the northern high latitudes detected from multi-satellite data’, *Environmental Research Letters*, 6(4), p. 045508. Available at: https://doi.org/10.1088/1748-9326/6/4/045508.